Spatio-Temporal Analysis Tool for Modeling Pulmonary Nodules in MR Images

Li Shen[a], Heng Huang[b], James Ford[b], Chia-Hsin Lu[a],
Ling Gao[c], Wei Zheng[b], Fillia Makedon[b], Justin Pearlman[c]

[a]Image and Pattern Analysis Laboratory, Department of Computer and Information Science, University of Massachusetts Dartmouth, North Dartmouth, MA 02747, USA
[b]Dartmouth Experimental Visualization Laboratory, Department of Computer Science, Dartmouth College, Hanover, NH 03755, USA
[c]Advanced Imaging Center, Departments of Radiology and Cardiology, Dartmouth Medical School, Lebanon, NH 03756, USA

ABSTRACT

To detect lung cancer at an earlier stage, a promising method is to apply perfusion magnetic resonance imaging (pMRI) modified to assess tumor angiogenesis. One key issue is to effectively characterize angiogenic patterns of pulmonary nodules. Based on our previous study addressing this issue, in this work, we develop STAT, a Spatio-Temporal Analysis Tool that implements not only our previously proposed pulmonary nodule modeling framework but also a user friendly interface and many extended functions. Our goal is to make STAT an easy-to-use tool that can be applied to more general cases. STAT employs the following overall strategy for modeling pulmonary nodules: (1) nodule identification using a correlation maximization method, (2) nodule segmentation using edge detection, morphological operations and model-based strategy, and (3) nodule registration using landmark approach and thin-plate spline interpolation. In nodule identification, STAT provides new schemes for selecting the template and refining results in difficult cases. In nodule segmentation, STAT provides additional flexibilities for creating the weighting mask, selecting morphological structure elements and individually fixing segmentation result. In nodule registration, our previous study uses principal component analysis for landmark extraction, which may not work in general. To overcome this limitation, STAT provides an enhanced approach that minimizes the bending energy of the thin plate spline interpolation or mean square distance between each landmark set and the template set. Our main application of STAT is to define blood arrival patterns in the lung to identify tumor angiogenesis as a means of early accurate diagnosis of cancer.

Keywords: Perfusion MRI, pulmonary nodule, segmentation, registration

1. INTRODUCTION

Lung cancer is among the most commonly occurring malignancies in the world and is the leading cause of cancer death in both men and women in the US. Computed tomography (CT) can identify suspicious lesions, but its high false-positive rate often requires additional imaging tests within 3-6 months to confirm a positive result. To detect lung cancer at an earlier stage, an alternative and promising method is to apply perfusion magnetic resonance imaging (pMRI)[1] modified to assess tumor angiogenesis. Angiogenesis is one of the most promising areas in cancer research. It is defined as the formation and development of new blood vessels, essential for tumor growth and the eventual spread of cancer cells to secondary locations throughout the body.

Send correspondence to Li Shen. E-mails: lshen@umassd.edu, heng.huang@dartmouth.edu, jford@cs.dartmouth.edu, g_clu@umassd.edu, {ling.gao, wei.zheng, fillia.makedon, justin.pearlman}@dartmouth.edu

One key issue in the analysis of pMRI lung image sequences is to effectively characterize angiogenic patterns of pulmonary nodules. Many techniques of nodule detection (*e.g.,* Lee 2001[2]) and segmentation (*e.g.,* Xu 2002[3]) have been developed based on chest radiographs or CT images. New challenges arising in the analysis of pMRI sequences include the following: (1) as a different imaging modality, pMRI requires new processing techniques for detection and segmentation of lung nodules, and (2) to compensate for respiratory and cardiovascular motion in pMRI sequences, registration needs to be done to ensure the corresponding nodule occurrences in different time frames to be comparable.

We have investigated this problem in a prior study[4] and proposed an automated spatio-temporal modeling framework for pulmonary nodules in pMRI sequences. The resulting spatio-temporal model can lead to many types of nodule characterization, *e.g.*, a time intensity profile of a nodule region; and be used to capture important angiogenic patterns in the lung that can distinguish between cancer and benign nodules and help early detection.

To make full use of the technique, in this work, we develop STAT, a Spatio-Temporal Analysis Tool that implements not only the previously proposed framework but also a user friendly interface and many extended functions. Our goal is to make STAT an easy-to-use tool that can be applied to more general cases. We describe our method using real pMRI image sequences in Section 2, present sample results in Section 3, and conclude the paper in Section 4.

2. METHODS

We first describe the image data used in this study, next present the STAT interface and its overall strategy, and then discuss each processing step in details. These steps include identification, segmentation, and registration.

2.1. Image data

Prior written consent was obtained as approved by the hospital research board. Surface EKG electrodes were used for cardiac cycle timing during the MR imaging procedure. MR imaging was performed using an eight-channel phased-array coil of a 1.5-T whole-body GE dual gradient Excite magnet. After scout images of the chest a bolus Fast Gradient-Echo Train imaging (FGRET) was performed at the rate of one image per heartbeat with flip angle adjusted to null the target lesion on fourth and subsequent frames prior to arrival of contrast agent (TR/TE/flip angle = 6.06 ms/1.108 ms/75^o, views per segment = 4, matrix = 256×256, field of view = 440×440 mm, EKG triggered RR = 1). Likewise, static inversion recovery images were adjusted to null the target lesion, typically using TI = 250-300 msec. While imaging by FGRET, 20 ml of Gd-DTPA (Magnevist, Berlex Laboratories) was injected into the venous line as a time series of 80-84 images were obtained at one frame per heartbeat observing signal changes relating to arrival and washout of the contrast agent. Subsequently, at 5, 10, and 15 minutes after injection, delayed enhancement static inversion recovery images were obtained to assess agent retention (which occurs in damaged cells). In this study, we process the time series of images obtained during the first-pass of the bolus of contrast agent to demonstrate our spatio-temporal modeling technique and tool. Figure 2 shows three examples from one series of 80 images.

2.2. STAT interface

STAT follows the overall strategy proposed in our prior study,[4] which is to divide the problem into several relatively simple subproblems. Generally speaking, image registration[5] is a difficult task. However, if we localize relevant nodule region that is actually our focus, registration of this sub-image between different time frames becomes a much easier task. More conveniently, we can even extract the nodule boundary from this sub-image, and then use the segmentation results to complete nodule registration.

Thus, our framework includes 3 steps: (1) nodule identification in each slice, (2) nodule segmentation in the relevant region, and (3) nodule registration using segmentation results. These steps are described in more details in the following subsections, where we also describe how the STAT tool extends our prior work.

The interface of STAT consists of a control panel and an image browser, see Figure 1. The slider on the control panel can be used to browse a series of lung images or localized nodule regions. Push buttons are used to open image sequences, save processing results, and initiate processing steps such as nodule identification, nodule segmentation, landmark extraction, and nodule registration. Edit boxes are used to adjust different parameters

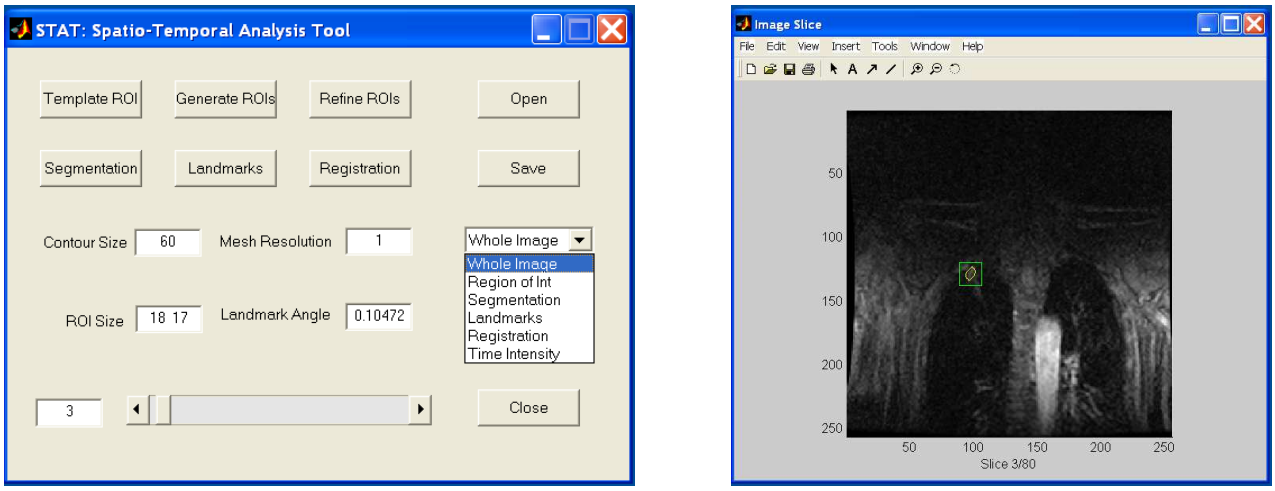

(a) Control panel (b) Image browser

Figure 1. The interface of STAT consists of a control panel and an image browser. The slider on the control panel can be used to browse a time series of lung images or nodule slices. The popup menu can be used to view results generated at different processing stages. Push buttons are used to open image sequences, save processing results, and initiate processing steps. Edit boxes are used to adjust different parameters used in the tool.

used in the tool. The popup menu can be used to view intermediate or final results generated at different processing stages. We briefly describe the menu items as follows.

- Whole Image: A complete image in the sequence is rendered in the image browser. If available, a nodule region and a nodule boundary are also marked on the image. See Figures 1(b), 2 and 9 for a few examples.
- Region of Int: A localized region of interest (ROI) is zoomed in and rendered in the browser. This ROI should contain a nodule of interest, which is the result of nodule identification. The visualization for this option is similar to examples shown in Figure 5 if those nodule boundaries (green contours) are excluded.
- Segmentation: This is similar to the "Region of Int" visualization. But the nodule boundary is also shown in the browser. See Figure 5 for a few examples.
- Landmarks: This is similar to the "Segmentation" visualization. But a set of automatically extracted landmarks are also shown in the browser. See Figure 6 for a few examples.
- Registration: This is similar to the "Landmarks" visualization. In addition, a mesh is superimposed onto the image to show the registration result. See Figure 7 for a few examples.
- Time Intensity: A mean time intensity curve for a specified region (by default, the current nodule) is plotted in the browser. See the last plot in Figure 9 for an example, where three curves are integrated into one plot.

2.3. Identification

To identify a local nodule region in each image slice, we employ a simple method as follows. In one slice, we manually define a rectangular region A to enclose the nodule of interest. In other words, A is an $m \times n$ sub-image that contains the nodule. In each of the other slices, we search for a region B of the same size that maximizes the correlation coefficient between A and B. The two-dimensional correlation coefficient between two matrices A and B of the same size is given by the formula

$$r = \frac{\sum_m \sum_n (A_{mn} - \bar{A})(B_{mn} - \bar{B})}{\sqrt{(\sum_m \sum_n (A_{mn} - \bar{A})^2)(\sum_m \sum_n (B_{mn} - \bar{B})^2)}},$$

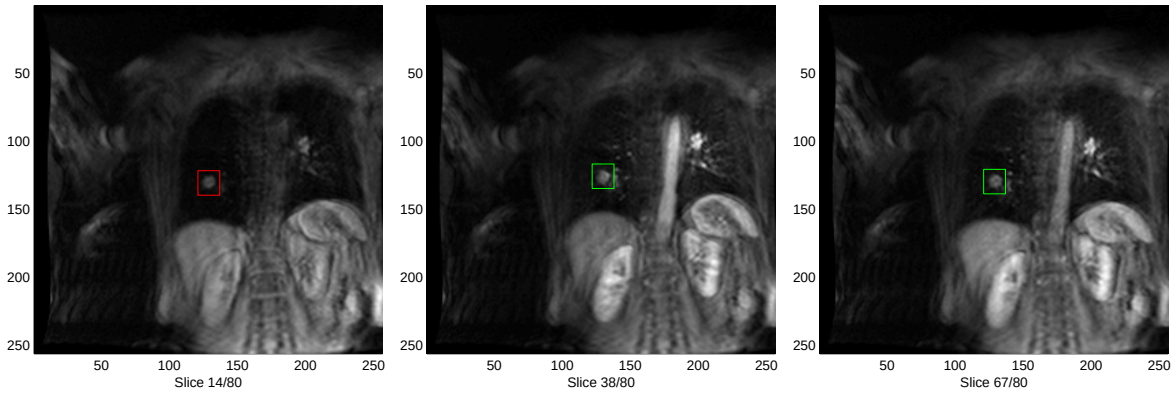

Figure 2. Sample nodule identification: users define a rectangular region A to enclose the nodule of interest in one frame (see red box in the left image); in each other frame (see green boxes in the middle and right images), STAT automatically searches for a region B of the same size that maximizes the correlation coefficient between A and B.

where $\bar{X}$ denotes the mean of the elements of matrix X.

In our implementation, after initializing B to have the same location as A, we move B in the neighborhood area, calculate the correlation coefficient for each case, and then select the best one. Although this is a simple approach, it works perfectly on our data. The nodule region is correctly identified in all the slices. Figure 2 shows three sample image slices with identified nodule regions.

For convenience, we say that A is our template region of interest (ROI), or simply the *template*. STAT implements the above approach in an interactive manner. Using the image browser, a user can pick an image slice and manually trace a template ROI on it. After clicking "Generate ROIs" button on the control panel, nodule regions can be identified automatically for all the other slices. In STAT, the template ROI is colored in red and nodule regions on all the other slices are in green (Figure 2) so that users can distinguish between them.

Besides the above basic function, STAT provides a few more functions for users to deal with difficult cases. First, a user can click the "Template ROI" button to modify the ROI on the current slice and make it as the template. This is especially helpful if the ROI on a neighboring slice is out of focus. In this case, a correct nodule region can often be identified after generating all nodule regions using the new template.

Second, in STAT, the size of the neighborhood area covered by the search for B can be customized by users. For different image sequences, their nodule sizes may vary a lot. Thus, a customized definition of neighborhood area can not only save the processing time but also produce better results.

Third, a user can click the "Refine ROIs" button to refine the current nodule region. In this case, the search starts from the current nodule location instead of the template location and then explores the corresponding neighborhood area. This option can help refine the result iteratively until a desired one is obtained.

Finally, STAT also allows a user to manually modify the nodule region on each slice. This option is provided for the worst case and we don't expect it will be frequently used.

2.4. Segmentation

Nodule segmentation is performed on each sub-image or ROI identified in the previous step, which reduces the complexity of segmentation. Figure 5 shows sample nodule sub-images (ignore the segmentation results in these images for now). The nodule appearance in these sub-images is relatively clear. Thus, a few simple image processing techniques can be combined to complete the segmentation task.

We first design a segmentation procedure as follows: (1) Apply a filter to reduce contribution of noise, *e.g.*, 3×3 average, median, or median-average filter (average used in our experiments); (2) apply Canny edge detection to extract object edges; (3) if necessary, close the object edges to form a simply-connected object, using an approach described in the next paragraph. The Canny method used in the second step finds edges by looking

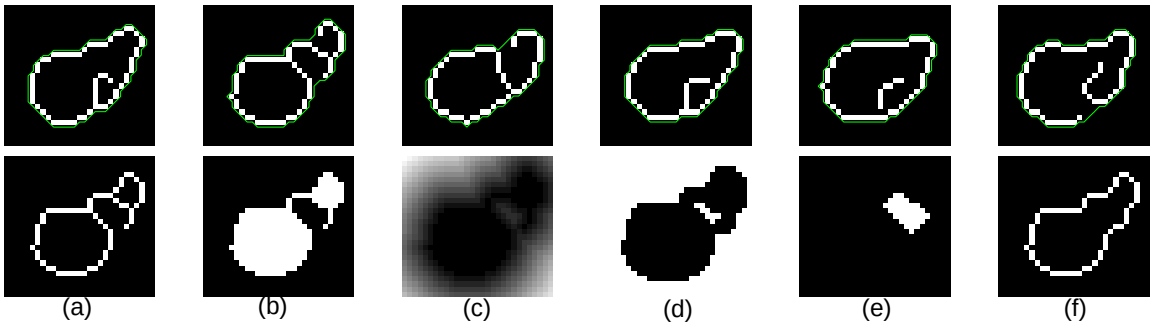

Figure 3. Nodule boundary segmentation. The first row shows sample edge detection results (write pixels) and segmentation results (green contours). The second row shows a sample procedure of closing broken edges: **(a)** initial edges, **(b)** bridge unconnected pixels and fill image region, **(c)** distance transformation map (DTM), **(d)** threshold DTM and find connected components, **(e)** remove the background component and slightly dilate the rest of the components, and **(f)** extract the boundary of (b)+(e).

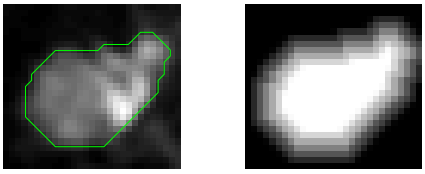

Figure 4. Mean nodule image (left), mean nodule boundary (green contour), and weighting mask (right).

for local maxima of the gradient of the image. The gradient is calculated using the derivative of a Gaussian filter. The method uses two thresholds, to detect strong and weak edges, and includes the weak edges in the output only if they are connected to strong edges. This method is known to many as the optimal edge detector.

The first row of Figure 3 shows six sample results after performing the first two steps of the segmentation procedure. Some of these results (a, d and e) form a closed nodule region, while others (b, c and f) do not. The third step is designed as follows to derive a closed nodule boundary: **(a)** start from the edge detection result; **(b)** bridge previously unconnected pixels (works only for small gaps) and then fill image regions; **(c)** calculate the distance transformation map; **(d)** threshold the transformation map ($t = 1.5$ in this example), find its connected components, and make the background form a single connected component; **(e)** remove the background component and slightly dilate the rest components (a radius=3 disk used as the morphological structuring element in this example); and **(f)** add the results of (b) and (e) and extract its boundary. The second row of Figure 3 shows a sample run of the above procedure.

The above segmentation procedure works for most of nodule sub-images. However, for some noisy cases, it fails to create a reasonable nodule shape. To overcome this problem, we introduce a weighting mask to capture a general nodule shape and then apply it to each image to impose some structural constraint on the segmentation results. We use the following approach to calculate the weighting mask: (1) scale the intensity values to the range from 0 (black) to 1 (white) for each sub-image, and calculate the mean image; (2) segment the mean using the procedure described above; (3) calculate the signed distance transformation map of the mean boundary; and (4) threshold the transformation map so that the most positive and negative values become t and $-t$ respectively ($t = 3$ in this example).

Figure 4 shows the mean nodule boundary and the weighting mask. Since the weighting mask captures a general nodule shape, we multiply it to each nodule image on a pixel-by-pixel basis and then perform segmentation as described before. Clearly, this approach imposes structural constraint on each individual nodule so that its shape won't deviate too much away from a typical nodule shape. Using this strategy, we obtain satisfactory results for all the image sequences used in this study. Figure 5 shows some of the results.

STAT implements the above approach and provides additional flexibilities: (1) users can specify the set of

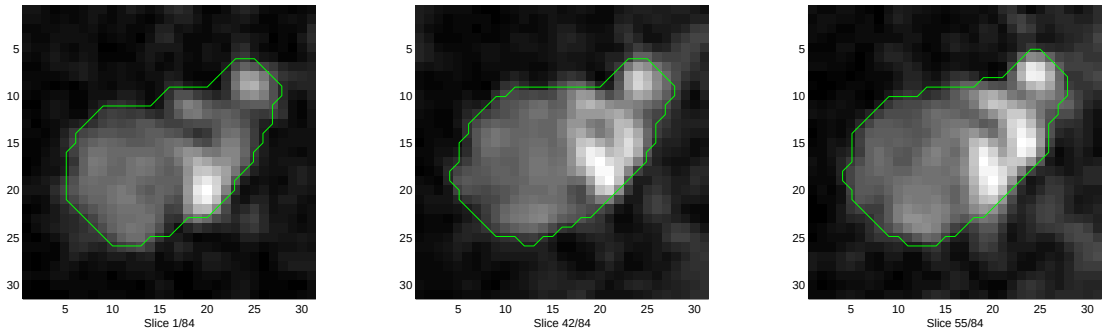

Figure 5. Sample segmentation results: green contour shows the nodule boundary

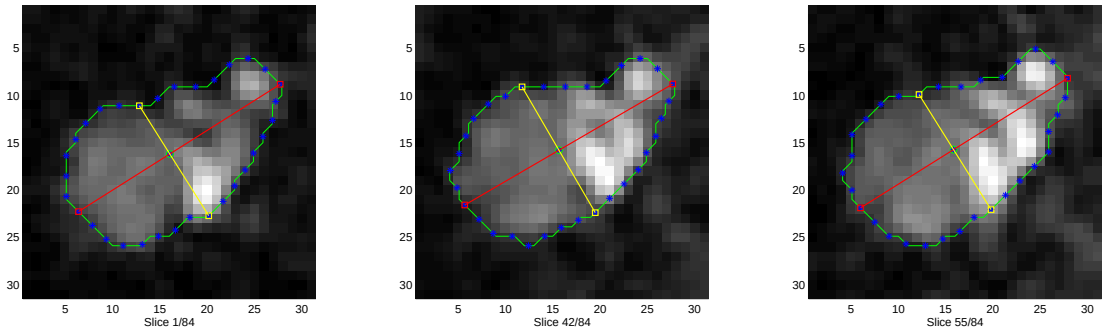

Figure 6. Landmark extraction: blue stars are extracted landmarks.

images used to create the weighting mask; (2) structure elements are adjustable for morphological processing; (3) segmentation result on a specific image can be fixed individually, using either manual tracing or automatic method by adjusting the weighting image; (4) a user-specified contour size can be adjusted to make sure the segmentation result is indeed the nodule rather than other noisy objects in the image; and (5) the cutoff value for thresholding the distance transformation map is also adjustable.

2.5. Registration

After segmentation, the spatial characteristics of a nodule are available at each time point. To build a spatio-temporal nodule model, we need to complete the registration along the temporal dimension. In other words, for each pixel inside the nodule in a user-specified slice, we need to find its corresponding pixels in all the other slices. We develop a landmark-based registration approach, which includes automatic identification of landmarks in each slice and thin-pline spline interpolation[6] for image matching.

A landmark is a point of correspondence on each nodule occurrence that matches between time frames. In our prior study,[4] we have developed the following procedure to automatically extract a set of landmarks in each slice. We run principal component analysis (PCA)[7] to each nodule represented by a binary image to find its principal

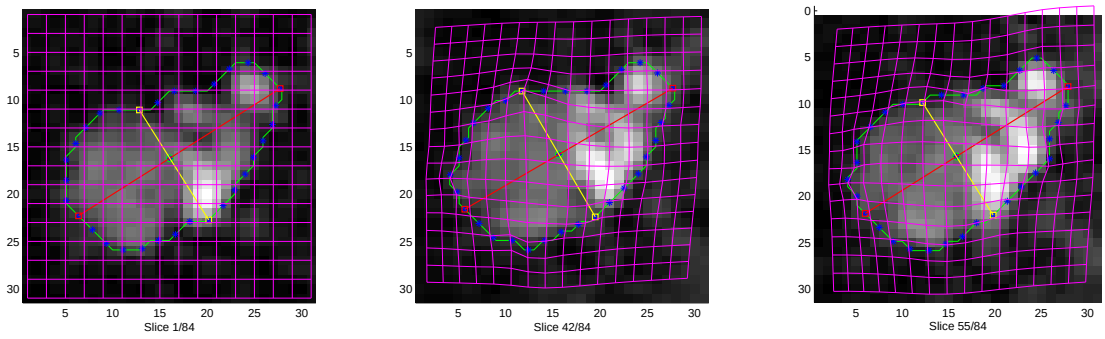

Figure 7. Sample registration results: the superimposed mesh shows the registration.

axes. These principal axes intersect the nodule boundary at four points, which become our base landmarks. We can then extract more landmarks by finding the midpoint of the contour between two neighboring landmarks and defining it as a new landmark. Besides these boundary landmarks, we also include the nodule centroid as an additional landmark. Figure 6 shows the PCA axes and sample landmarks. These are labeled landmarks, which are consistent across subjects. In the following, we first introduce the landmark-based registration, and then discuss several additional schemes implemented in STAT for better extraction of landmarks.

Landmarks define the correspondence at the nodule boundary and centroid. To create correspondence for the interior part, we employ thin-plate spline interpolation.[6] A thin-plate spline $f(x, y)$ is a smooth function which interpolates a surface that is fixed at the landmark points P_i at a specific height h_i. If one imagines this surface as a thin metal plate, then this plate will take a shape in which it is least bent, *i.e.*, it minimizes the bending energy of $f(x, y)$:

$$E(f) = \int\int_{R^2} (\frac{\partial^2 f}{\partial x^2})^2 + (\frac{\partial^2 f}{\partial x \partial y})^2 + (\frac{\partial^2 f}{\partial y^2})^2 \, dx \, dy.$$

In order to map one image to another using landmark data, we compute two of these spline surfaces, one (f_x) in which the heights (h_i's) are loaded with the x-coordinate of the landmarks (P_i's) in the second image, another (f_y) for the y-coordinate. Then the first of these functions supplies the interpolated x-coordinate of the map we seek, and the second the interpolated y-coordinate. The resulting map ($f_x(P)$, $f_y(P)$) is now a deformation of one image plane onto the other which maps landmarks onto their homologues and has the minimum bending energy of any such interpolant. Figure 7 shows sample results of applying thin-plate spline interpolation to our data. Clearly, given any nodule pixel in the template slice, now we can find the corresponding pixels in all the other slices. Thus, nodule registration across different time frames can be achieved.

Note that STAT shows the registration results by superimposing a mesh onto an image (see Figures 7 and 8), where the mesh resolution can be adjusted in order to get the best visualization. As we have mentioned before, STAT provides several additional schemes for landmark extraction, since the PCA approach does not work in general. For example, if a nodule has a round shape, it will be difficult to find its principal axis using PCA. To overcome this limitation, STAT provides three alternative approaches, which are grouped under a popup menu in the control panel shown in Figure 8(a).

Either of the first two approaches aims to minimize an objective function defined based on a landmark set and the template set: (1) one approach minimizes the mean square distance (MSD) between these two landmark sets; and (2) the other minimizes the total bending energy (BE) of the thin-plate spline interpolation between them. The total bending energy between two landmark sets are calculated as the sum of $E(f_x)$ and $E(f_y)$, where f_x is the spline surface for interpolating x coordinates and f_y is the surface for y coordinates.

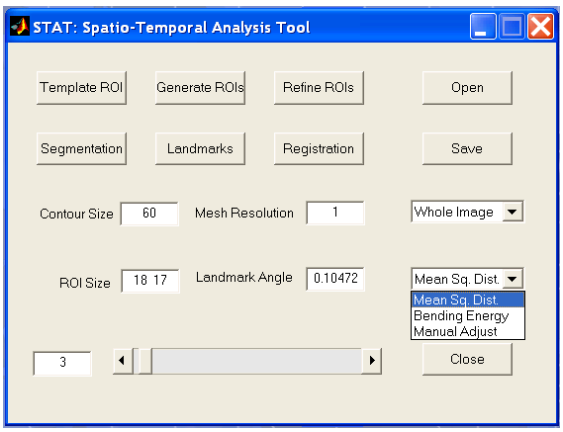

(a) Landmark extraction options

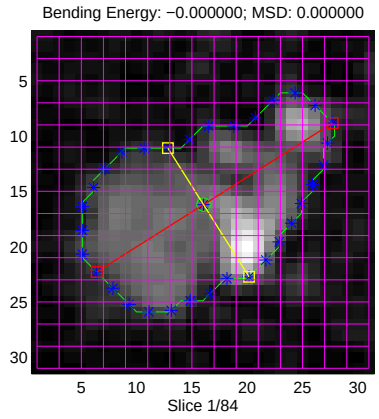

(b) Landmarks on the template slice

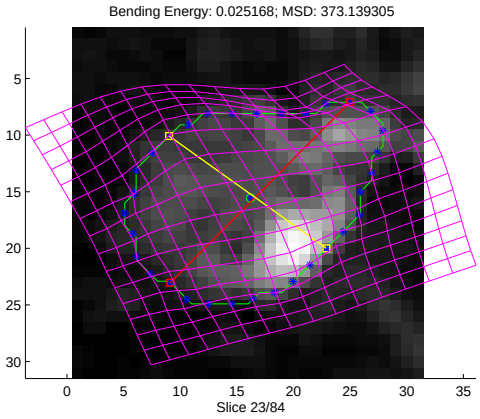

(c) Landmarks on Slice 23

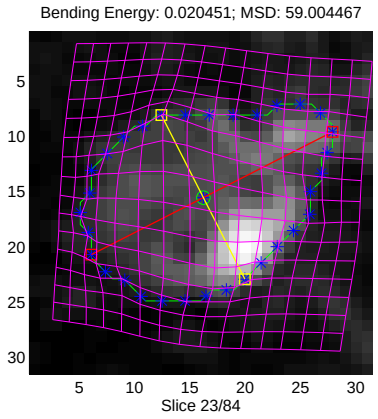

(d) Rotated version of (c)

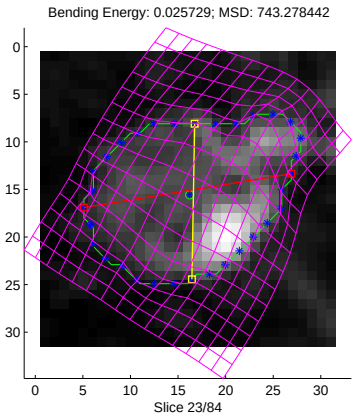

(e) Rotated version of (d)

Figure 8. (a) Three additional schemes for landmark extraction, which are grouped under a popup menu in the control panel. **(b)** Landmarks on the template slice, to which all the other image slices are registered. **(c-e)** Sample landmark rotation on a typical nodule slice: (1) each plot contains the same set of landmarks, (2) the red and yellow axes indicates the landmark correspondence to the template (shown in (b)), and (3) according to the axes the landmark correspondence is rotated in a clockwise direction from (c) to (e). On each nodule slice, STAT also shows the values of the mean square distance (MSD) and the bending energy (BE) of the thin-plate spline interpolation between the current landmark set and the template set.

Since the number of landmarks is not large due to the small size of a nodule, we use an exhaustive search approach to achieve both minimizations by rotating landmarks along the nodule boundary. Figure 8(c-e) shows sample landmark rotations on a typical nodule slice: (1) each plot contains the same set of landmarks, (2) the red and yellow axes indicate the landmark correspondence to the template shown in Figure 8(b), and (3) according to the axes the landmark correspondence is rotated in a clockwise direction from (c) to (e). For each rotated correspondence, we can examine its BE and MSD values and then find the minimal ones over all possible rotations. A user can also specify the number of landmarks used in the analysis to adjust the sampling resolution for each minimization.

In the worst case, STAT offers the third approach, which is to allow users to manually fix the landmark assignment by rotating landmarks along the nodule boundary. This is the advantage that an interactive tool can provide. For example, Figure 8(c-e) shows some sample landmark rotations on a typical nodule slice. In addition, on each nodule slice, STAT also shows the values of the mean square distance (MSD) and the bending energy (BE) of the thin-plate spline interpolation between the current landmark set and the template set. Thus,

by looking at these values, a user can rotate the landmark set manually for any particular slice and then pick a satisfactory result. We do not expect this function to be used very often. However, it is convenient to have this function available and it can be used to deal with some difficult cases.

3. RESULTS

We have used STAT to analyze several image sequences, each of which comprises $80-84$ lung perfusion, short-axis, MR images obtained from freely breathing patients. See Section 2.1 for a brief description of the image acquisition procedure. Figure 1 shows the interface of the STAT tool. Figure 2 shows sample nodule identification results. Figures 5, 6 and 7 show sample results of segmentation, landmark extraction and registration, respectively. After these steps, a spatio-temporal model is established for the nodule.

Using this model, STAT can create a time intensity profile for any region in the nodule. Such a region can be specified in any slice. According to our model, the corresponding region in all the other slices can be easily extracted. Thus a time intensity profile for the specified region could be created as a curve showing mean intensity (or intensity variance) change over time.

Figure 9 shows sample time intensity profile results, where the mean intensity for the whole nodule is plotted over time. These time intensity profiles can capture different types of angiogenic patterns of the pulmonary nodule and have the potential in distinguishing cancer nodules from benign ones. Work is in progress to collect and process more cases in order to achieve this goal.

4. CONCLUSIONS

Based on our previous work,[4] we have developed STAT, a spatio-temporal analysis tool for modeling pulmonary nodules in pMRI image sequences. STAT extends our previous study by creating an easy-to-use interface as well as incorporating many new functions. STAT can be used to extract motion-tracked time intensity profiles for any user-interested nodule regions. This spatio-temporal model also supports other types of nodule characterization, *e.g.*, volume/shape change over time. Our main application of this model is to define blood arrival patterns in the lung to identify tumor angiogenesis as a means of early accurate diagnosis of cancer. One future direction is to incorporate into STAT new components for pattern analysis of time intensity profiles.

ACKNOWLEDGMENTS

This work was supported by the Flight Attendant Medical Research Institute.

REFERENCES

1. C. Fink, M. Puderbach, *et al.*, "Regional lung perfusion: assessment with partially parallel three-dimensional MR imaging," *Radiology* **231**(1), pp. 175–84, 2004.
2. Y. Lee, T. Hara, H. Fujita, *et al.*, "Automated detection of pulmonary nodules in helical CT images based on an improved template-matching technique," *IEEE Trans. on Medical Imaging* **20**, pp. 595–604, 2001.
3. N. Xu *et al.*, "Automated lung nodule segmentation using dynamic programming and EM based classification," in *SPIE Medical Imaging*, **4684-70**, 2002.
4. L. Shen, W. Zheng, L. Gao, H. Huang, F. Makedon, and J. Pearlman, "Spatio-temporal modeling of lung images for cancer detection.," *Oncology Reports, Special Issue on Computational Analysis and Decision Support Systems in Oncology* , 2006, in print.
5. J. Maintz and M. Viergever, "A survey of medical image registration," *Medical Image Analysis* **2**, pp. 1–36, 1998.
6. F. Bookstein, "Principal warps: Thin-plate splines and the decomposition of deformations.," *IEEE Trans. on Pat. Ana. and Mac. Int.* **11**(6), pp. 567–585, 1989.
7. R. O. Duda, P. E. Hart, and D. G. Stork, *Pattern Classification (2nd ed)*, Wiley, New York, NY, 2000.

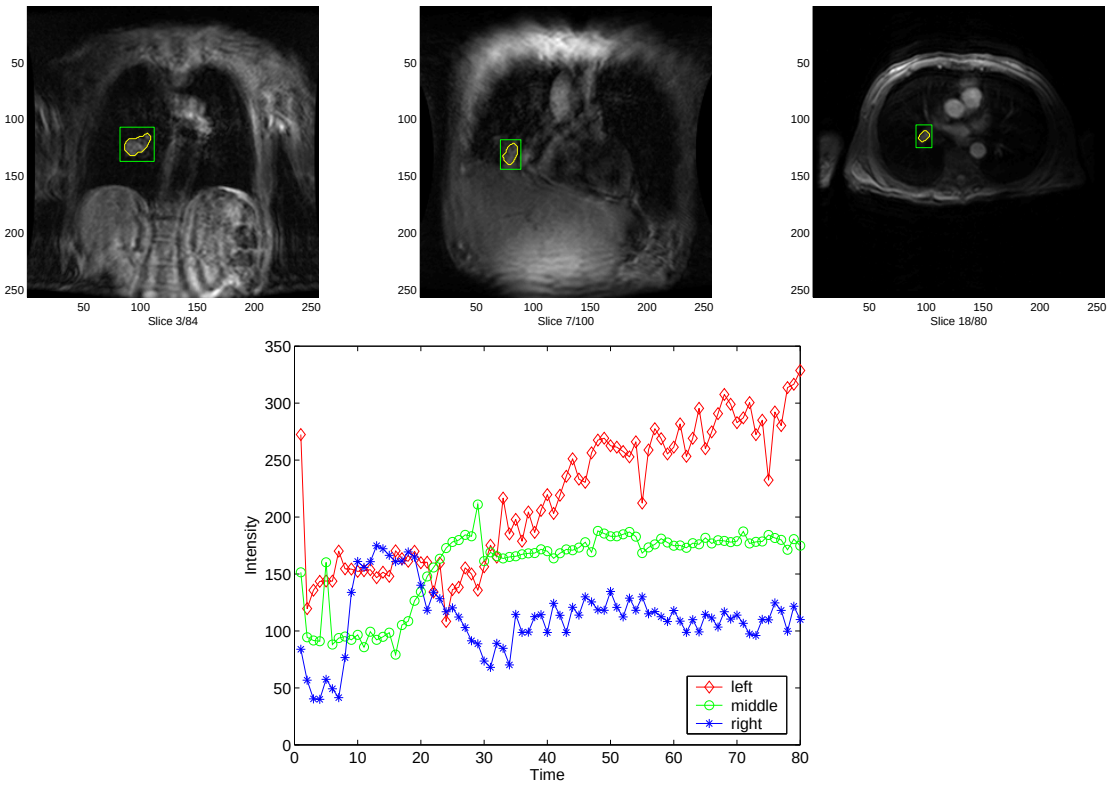

Figure 9. Time intensity profile results. The top row shows sample image slices of two cancer nodules (left and middle) and one benign nodule (right). The bottom row shows their time intensity profiles.